

## Spectral method for determining mean dissipation rates of turbulent kinetic energy and passive scalar variance

S. K. Lee, L. Djenidi and R. A. Antonia

School of Engineering, The University of Newcastle, N.S.W., 2308 AUSTRALIA

### Abstract

Mean dissipation rates  $\langle \varepsilon \rangle$  and  $\langle \chi \rangle$  of the turbulent kinetic energy and of a passive scalar are important in the theory and modelling of turbulent mixing. In reality, turbulence is usually not isotropic. Twelve velocity derivatives and three scalar derivatives are required to compute these quantities, and so the estimate of the dissipation rates presents a real challenge. We overcome this by developing a spectral method that is tenable for a wide range of Taylor microscale Reynolds numbers provided the small scales are not adversely affected by flow inhomogeneities. The method applies to turbulent mixing for a Prandtl number close to unity and excludes near-wall turbulence. It involves juxtaposing a series of calibrated reference spectra at increments of  $\Delta\langle \varepsilon \rangle$  and  $\Delta\langle \chi \rangle$  to the measured spectra to identify the best match. The technique is demonstrated by applying it to previously published grid turbulence data.

### Introduction

This paper presents an empirical method to estimate the mean turbulent kinetic energy (TKE) and scalar variance dissipation rates,  $\langle \varepsilon \rangle$  and  $\langle \chi \rangle$  respectively, for turbulent mixing at a Prandtl number close to unity. This work extends Djenidi and Antonia's (D&A) [5] "spectral chart" method of estimating  $\langle \varepsilon \rangle$  to include the estimate of  $\langle \chi \rangle$  for a passive scalar. The D&A method relies on the assumption that the dissipative end of the spectrum scales on  $\langle \varepsilon \rangle$  and the kinematic viscosity  $\nu$ . This assumption is valid for large values of the Taylor microscale Reynolds number  $R_\lambda (= \lambda u'/\nu; \lambda$  is the Taylor microscale and  $u'$  is the streamwise velocity fluctuation; a prime denotes the root-mean-square value) as postulated in the similarity hypothesis of Kolmogorov [6], but is equally tenable at small/moderate  $R_\lambda$  provided any inhomogeneities in the flow do not affect the dissipative scales [5]. The extension of the method to a passive scalar is straightforward — the dissipative end of the spectrum is assumed to scale on  $\langle \varepsilon \rangle$ ,  $\nu$  and  $\langle \chi \rangle$ . This assumption is tenable at large  $R_\lambda$ , as enunciated in Obukhov's [11] similarity hypothesis, but should hold at small/moderate  $R_\lambda$ .

The present method applies to the lower wavenumber region of the dissipation range that is less susceptible to electronic noise and imperfect spatial/temporal resolution of the measurement probe(s). It does not have to rely on the presence of a "−5/3" inertial range associated with large  $R_\lambda$  [6], and no calculations of velocity or scalar derivatives are required [5]. For convenience, a "Pope" model spectrum [12] may be used to calibrate with a reliable reference spectrum — either from direct numerical simulations (DNS) or from sufficiently well resolved measurements, as discussed in [5]. The model spectrum is then plotted in dimensional form to provide the clearest comparison with the measured spectrum. By identifying the model spectrum that most closely matches the measured spectrum in the dissipation range, the actual value for the mean dissipation rates can be easily determined [5]. In the following sections, the method is described in more detail and tested against available grid turbulence data. The test is by no means exhaustive but serves to demonstrate that the technique is robust.

### The mean dissipation rates

In turbulent mixing, the mean dissipation rates for the TKE and the scalar variance are defined by the following *tensorial* forms

$$\langle \varepsilon \rangle = (1/2)v\langle (\partial u_i/\partial x_j + \partial u_j/\partial x_i)^2 \rangle, \quad (1)$$

$$\langle \chi \rangle = \kappa\langle (\partial \theta/\partial x_i)^2 \rangle, \quad (2)$$

where  $\kappa$  is the scalar diffusivity. The mean TKE is defined as  $q^2 = u'^2 + v'^2 + w'^2$  ( $u$  is the streamwise component of velocity fluctuation;  $v$  and  $w$  are the cross-stream components) and the scalar variance is  $\theta'^2$ . For "isotropic" turbulence, (1) and (2) simplify to the following expressions

$$\langle \varepsilon_{\text{iso}} \rangle = 15\nu\langle (\partial u/\partial x)^2 \rangle = 15\nu \int_0^\infty k_1^2 \phi_u(k_1) dk_1, \quad (3)$$

$$\langle \chi_{\text{iso}} \rangle = 3\kappa\langle (\partial \theta/\partial x)^2 \rangle = 3\kappa \int_0^\infty k_1^2 \phi_\theta(k_1) dk_1, \quad (4)$$

where  $\phi_u$  and  $\phi_\theta$  are the spectral densities for  $u$  and  $\theta$  respectively, and  $k_1$  is the one-dimensional wavenumber. For approximately isotropic grid turbulence [17], the mean dissipation rates are obtained from the transport equations for  $q^2$  and  $\theta'^2$ , i.e.

$$\langle \varepsilon_d \rangle = -(U_0/2)(dq^2/dx), \quad (5)$$

$$\langle \chi_d \rangle = -(U_0/2)(d\theta'^2/dx), \quad (6)$$

where the subscript "d" denotes measurements of  $\langle \varepsilon \rangle$  and  $\langle \chi \rangle$  obtained from the rates of decay of  $q^2$  and  $\theta'^2$  at a free-stream velocity of  $U_0$ . From their simultaneous measurements of all three components of velocity and scalar fluctuations, Zhou *et al.* [17] demonstrated that both sets of equations yield nearly the same results for grid turbulence, i.e. the ratios  $\langle \varepsilon_d \rangle/\langle \varepsilon_{\text{iso}} \rangle$  and  $\langle \chi_d \rangle/\langle \chi_{\text{iso}} \rangle$  are  $\approx 1 \pm 0.1$ .

### The power spectra

According to Kolmogorov's [6] similarity hypothesis, the normalised streamwise velocity ( $u$ ) spectrum may be represented as a universal function of the form

$$f_u(k_1 \eta) = \frac{\phi_u(k_1)}{\nu^{5/4} \langle \varepsilon \rangle^{1/4}} = \frac{\phi_u(k_1)}{u_\kappa^2 \eta}, \quad (7)$$

where  $\eta = \nu^{3/4} / \langle \varepsilon \rangle^{1/4}$  and  $u_\kappa = \nu^{1/4} \langle \varepsilon \rangle^{1/4}$  are the respective Kolmogorov length and velocity. When a passive scalar is introduced in a stream, it does not affect the dynamics of the flow. For a Prandtl number ( $Pr = \nu/\kappa$ ) close to unity, the normalised scalar ( $\theta$ ) spectrum may be expressed as a universal function [4, 11]

$$f_\theta(k_1 \eta) = \frac{\phi_\theta(k_1)}{\nu^{5/4} \langle \varepsilon \rangle^{-3/4} \langle \chi \rangle} = \frac{\phi_\theta(k_1)}{\theta_\kappa^2 \eta} \quad (8)$$

with the scalar variable  $\theta_\kappa = \langle \chi \rangle^{1/2} \nu^{1/4} / \langle \varepsilon \rangle^{1/4}$ . Provided  $R_\lambda$  is very large ( $\gtrsim 10^3$ ) and the flow is reasonably independent of  $\nu$ , (7) and (8) may be written in the *compensated* forms [8]

$$\frac{\phi_u(k_1)}{\langle \varepsilon \rangle^{2/3} k_1^{-5/3}} = C_u^+ (k_1 \eta)^{5/3 - m_u}, \quad (9)$$

$$\frac{\phi_\theta(k_1)}{\langle \varepsilon \rangle^{-1/3} \langle \chi \rangle k_1^{-5/3}} = C_\theta^+ (k_1 \eta)^{5/3 - m_\theta}, \quad (10)$$

which exhibit a “ $-5/3$ ” power-law behaviour in the “inertial” or more vigorously “scaling” range. For  $m_u = m_\theta = 5/3$ , the respective Kolmogorov and Obukhov-Corrsin coefficients  $C_u^+$  and  $C_\theta^+$  may be considered quasi-universal [8]. As  $R_\lambda$  decreases ( $< 10^3$ ), the low-wavenumber end of the  $u$  and  $\theta$  spectra peels off from the “ $-5/3$ ” slope. This is accompanied by a narrowing of the scaling range and a departure of  $C_u^+$  and  $C_\theta^+$  from their universality [8].

It is well established that, for a wide range of  $R_\lambda$ , power spectra normalised by the Kolmogorov-type variables ( $\eta$ ,  $u_\kappa$  and  $\theta_\kappa$ ) exhibit reasonable collapse in both the higher wavenumber region of the scaling range ( $0.01 \lesssim k_1 \eta < 0.1$ ) and the lower region of the dissipation range ( $0.1 \lesssim k_1 \eta < 1$ ). While electronic noise and finite measurement resolution can prevent reliable estimates of the spectra at  $k_1 \eta \gtrsim 1$  [5], the adequacy of the Kolmogorov scaling is indirectly demonstrated by the fact that the second-order structure functions  $\langle (\delta u^*)^2 \rangle$  and  $\langle (\delta \theta^*)^2 \rangle$ , for example [2], collapse at small increments in the range  $1 \lesssim r^* \lesssim 10$ , where  $\delta \psi = \psi(x+r) - \psi(x)$  and  $\psi = u, \theta$  (an asterisk denotes normalisation by the Kolmogorov-type variables).

### Application of the spectral method

Since grid turbulence is sufficiently isotropic to allow simpler and more reliable estimates of  $\langle \varepsilon \rangle$  and  $\langle \chi \rangle$ , i.e. (3)–(6), the Kolmogorov normalised spectra (9) and (10) for grid turbulence should be reasonably accurate. In Figure 1(a), the measured spectra, like the DNS spectra reviewed by D&A [5], show adequate collapse in the range  $0.1 \lesssim k_1^* < 1$ . Figure 1(b) shows that, although there are fewer published scalar spectra for  $R_\lambda > 100$ , the spectra have a similar collapse in the same range of  $k_1^*$ . Note that, in Figure 1,  $\phi_u$  and  $\phi_\theta$  are weighted by  $k_1^2$  (i.e. the scaling range exhibits a “ $1/3$ ” power-law behaviour), this is so that we can more clearly observe the shape of the spectra in the dissipation range of the wavenumbers. For comparison, we included in Figure 1 some recently published spectra from the DNS data set of [1]. The simulation is for turbulent mixing in a channel flow at  $R_\lambda \approx 90$ ; high spatial resolution ( $\Delta x^* = 1.16$ ,  $\Delta y^* = 1.33$ ,  $\Delta z^* = 0.77$ ) allows extension of the spectra to slightly higher wavenumbers and precise determination of the mean dissipation rates. The Kolmogorov normalised DNS spectra are taken at the centreline with  $h^+ = u_\tau h / \nu = 1020$ , where  $u_\tau$  is the friction velocity,  $h$  is the half width of the channel and the superscript “+” denotes normalisation by wall units [1]. Note that all the spectra reproduced in Figure 1 are as obtained from the published literature. The fact that the  $u$  and  $\theta$  spectra collapse at the high wavenumbers reinforces the validity of the Kolmogorov-Obukhov-Corrsin scaling for a wide range of  $R_\lambda$ . It is thus possible to obtain a “model” of a universal spectrum for  $u$  and  $\theta$ . For the  $u$  spectrum, we use the analytical expression adapted from that outlined in D&A [5] and Pope [12], i.e.

$$\frac{\phi_u(k_1)}{u_\kappa^2 \eta} \equiv \phi_u^*(k_1^*) = (k_1^*)^{-5/3} f_u(k_1^*),$$

$$f_u(k_1^*) = C_{u1} \times \exp\{-C_{u2}[(k_1^{*4} + C_{u3}^4)^{1/4} - C_{u3}]\}, \quad (11)$$

where the coefficients  $C_{ui}$  ( $i = 1, 2$  and  $3$ ) are positive. Other alternatives such as the simplified ( $C_{u3} = 0$ ) exponential form  $f_u(k_1^*) = C_{u1} \times \exp\{-C_{u2}k_1^*\}$  and the “Pao” spectrum  $f_u(k_1^*) = C_{u1} \times \exp\{-(3/2)C_{u2}k_1^{*4/3}\}$  may be used but they offer less control of the curve fit [12]. To have the analytical model consistent for both the velocity and the passive scalar, we use the following expression for the  $\theta$  spectrum that is analogous to (11), i.e.

$$\frac{\phi_\theta(k_1)}{\theta_\kappa^2 \eta} \equiv \phi_\theta^*(k_1^*) = (k_1^*)^{-5/3} f_\theta(k_1^*),$$

$$f_\theta(k_1^*) = C_{\theta1} \times \exp\{-C_{\theta2}[(k_1^{*4} + C_{\theta3}^4)^{1/4} - C_{\theta3}]\}, \quad (12)$$

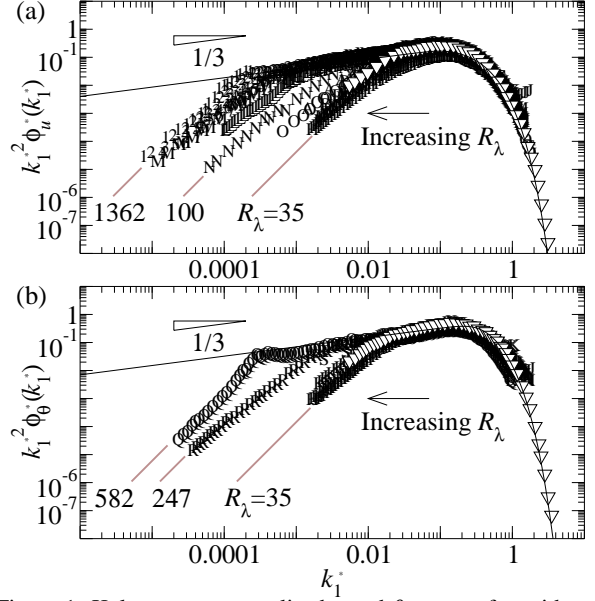


Figure 1: Kolmogorov normalised  $u$  and  $\theta$  spectra for grid turbulence using the (input) values  $\langle \varepsilon \rangle$  and  $\langle \chi \rangle$  reported in literature; for details of the symbols, see Table 1. For comparison, the DNS spectra ( $\nabla$ ) [1] taken at the centreline of a fully developed turbulent channel flow ( $h^+ = 1020$ ;  $R_\lambda \approx 90$ ) are used. For the solid black curves, (11) and (12) are used.

where the coefficients  $C_{\theta i}$  ( $i = 1, 2$  and  $3$ ) are also positive. Note that the functions  $f_u(k_1^*)$  and  $f_\theta(k_1^*)$  determine the shape of the spectra in the dissipation range only. In the inertial/scaling range ( $k_1^* < 0.1$ ), these functions are essentially unity so that the “ $-5/3$ ” power laws of the expressions (11) and (12) are recovered. To ensure a consistent treatment for all spectra reported in this work, the following coefficients, obtained by trial-and-error to minimise the least-squares difference between the model spectra and the “reference” (DNS) spectra in Figure 1, are kept constant, i.e.

$$C_{u1} = 0.4, \quad C_{u2} = 6.0 \quad \text{and} \quad C_{u3} = 0.1,$$

$$C_{\theta1} = 0.7, \quad C_{\theta2} = 5.5 \quad \text{and} \quad C_{\theta3} = 0.3.$$

The use of an analytical model offers a more clear cut approach to calibrating the reference spectra. Although it is just as valid to use *any* well resolved spectra, it is perhaps more convenient to implement the model coefficients since  $C_{ui}$  and  $C_{\theta i}$  can be easily updated to match the better resolved spectra.

Table 1 shows a collection of previously published data for  $R_\lambda = 35$  to  $1362$ , where the spectra, the mean dissipation rates and  $U_o$  are reported. The turbulence can be generated either by a passive grid or an active grid. Figure 2 shows the process of estimating the actual values  $\langle \varepsilon \rangle_N$  and  $\langle \chi \rangle_N$  by using the information given in Table 1. The initial estimates are taken from published values based on either isotropic assumptions (3) and (4) or decaying grid turbulence (5) and (6). From here, the estimated Kolmogorov (velocity) and Obukhov-Corrsin (scalar) variables can then be used to (un)normalise the spectra, viz.

$$\frac{2\pi}{U_o} f = k_1 = k_1^*/\eta, \quad (13)$$

$$\frac{U_o}{2\pi} \phi_\psi(f) = \phi_\psi(k_1) = \eta \phi_\psi(k_1^*) = \eta \psi_\kappa^2 \phi_\psi^*(k_1^*), \quad (14)$$

where  $\psi = u, \theta$ . By taking  $i$ -th iterations of  $\Delta\langle \varepsilon \rangle$  and  $\Delta\langle \chi \rangle$ , we obtain a family of model curves in juxtapositions to the measured spectra (Figure 3);  $\phi_\psi(f)$  is essentially used to avoid potential damping effect on  $\langle \varepsilon \rangle$  by the Kolmogorov scaling, e.g.  $\langle \varepsilon \rangle^{1/4}$ . In Table 1, the difference between the input value and

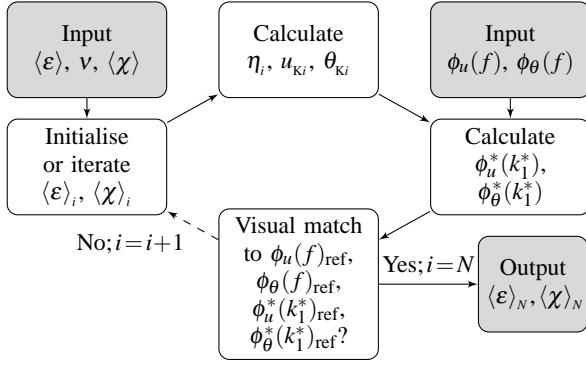


Figure 2: The spectral method uses an iterative process to estimate  $\langle \varepsilon \rangle_N$  and  $\langle \chi \rangle_N$ . Once there is a visual match between the measured and reference spectra, the process stops.

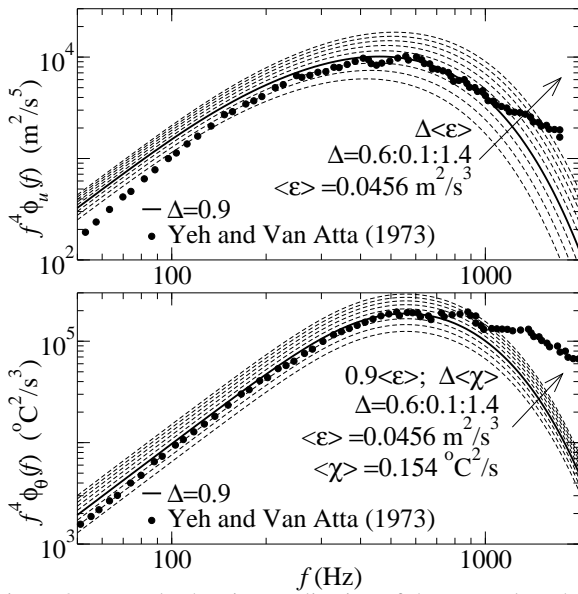


Figure 3: Example showing application of the spectral method to slightly heated grid turbulence data ( $\bullet R_\lambda = 35.2$ ) [16].

the output value for the mean dissipation rates is kept to a minimum, i.e.  $\Delta$  is kept as close to 1 as possible, while providing the best visual fit of the model curves to the measured  $u$  and  $\theta$  spectra in the dissipation range. Figure 4 shows that, by using  $\langle \varepsilon \rangle_N = \Delta \langle \varepsilon \rangle$  and  $\langle \chi \rangle_N = \Delta \langle \chi \rangle$  obtained from the spectral method, the Kolmogorov normalised  $u$  and  $\theta$  spectra exhibit a slightly better collapse in the dissipation range ( $0.1 \lesssim k_1 \eta < 1$ ). For the present review data (Table 1), the typical value of  $\Delta$  lies between 0.55 and 1.35. The extent of the departure from  $\Delta = 1$  may reflect the quality of the data or the uncertainty associated with estimating both the power spectra (using fast Fourier transform) and the mean dissipation rates. Possible factors contributing to the measurement uncertainty include contamination by electronic noise, imperfect resolution of the measurement probe(s) and non-negligible departures from isotropy. Given the uncertainty, the estimated values ( $\langle \varepsilon \rangle_N, \langle \chi \rangle_N$ ) remain close to those ( $\langle \varepsilon \rangle, \langle \chi \rangle$ ) published in the literature — the difference is  $\lesssim 45\%$  (Table 1). This should lend support to the validity of the spectral method and the universality of the model spectra (11) and (12) used to develop the method. This in turn implies that it would be worthwhile to assess the adequacy of the present technique on other turbulent flows, namely the mixing layer of jets and wakes, and geophysical turbulence.

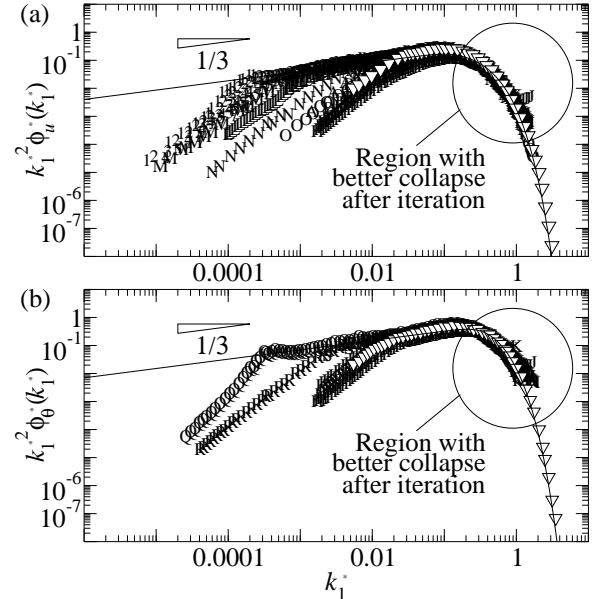


Figure 4: Kolmogorov normalised  $u$  and  $\theta$  spectra for grid turbulence using the iterated (output) values  $\langle \varepsilon \rangle_N$  and  $\langle \chi \rangle_N$ ; for details of the symbols, see Table 1.

### Concluding remarks

A simple method for determining the mean dissipation rates ( $\langle \varepsilon \rangle, \langle \chi \rangle$ ) in turbulent mixing has been presented and tested. The method essentially matches measured  $u$  and  $\theta$  spectra to universal spectra over the smaller wavenumber end of the dissipation range. The key assumption for the method is that the Kolmogorov-Obukhov-Corrsin (KOC) similarity holds for the dissipative scales even when  $R_\lambda$  is not very large ( $\geq 35$  for the present work). This is justifiable when the smallest scales of interest are not adversely affected by flow inhomogeneities. The method has the following advantages: (1) it uses the KOC scaling that is sufficiently robust and can be applied to (different) turbulent flows over a wide range of  $R_\lambda$ , (2) it provides immediate visual assessment of the quality of the measured spectra relative to the universal spectra, and (3) it avoids the need to calculate  $\langle \varepsilon \rangle$  and  $\langle \chi \rangle$  using any of the relations (1) to (6).

### Acknowledgement

Financial support from the ARC is gratefully acknowledged.

### References

- [1] Antonia, R. A. and Abe, H., Inertial range similarity for velocity and scalar spectra in a turbulent channel flow, in *Proc. 6th Turb. Heat Mass Transf.*, Begell House, Inc., 2009, 119–122, 119–122.
- [2] Antonia, R. A., Smalley, R. J., Zhou, T., Anselmetti, F. and Danaila, L., Similarity solution of temperature structure functions in decaying homogeneous isotropic turbulence, *Phys. Rev. E*, **69**, 2004, 016305.
- [3] Comte-Bellot, G. and Corrsin, S., Simple Eulerian time correlation of full- and narrow-band velocity signals in grid-generated, ‘isotropic’ turbulence, *J. Fluid Mech.*, **48**, 1971, 273–337.
- [4] Corrsin, S., On the spectrum of isotropic temperature fluctuations in an isotropic turbulence, *J. Appl. Phys.*, **22**, 1951, 469–473.

Table 1: Test of the spectral method using (slightly heated) grid turbulence data;  $\langle \varepsilon \rangle$  and  $\langle \chi \rangle$  are the previously published values;  $\langle \varepsilon \rangle_N = \Delta \langle \varepsilon \rangle$  and  $\langle \chi \rangle_N = \Delta \langle \chi \rangle$  are the iterated values obtained from the spectral method (Figure 2).

Reference	Input		$U_o$ (m/s)	$R_\lambda$ ( $= \lambda u / \nu$ )	Input		Output		Symbol
	$\phi_u, \phi_\theta$ spectrum	Grid flow Passive/Active (mode)			$\langle \varepsilon \rangle$ ( $\text{m}^2/\text{s}^3$ )	$\langle \chi \rangle$ ( $^\circ\text{C}^2/\text{s}$ )	$\langle \varepsilon \rangle_N$ ( $\text{m}^2/\text{s}^3$ )	$\langle \chi \rangle_N$ ( $^\circ\text{C}^2/\text{s}$ )	
Comte-Bellot and Corrsin [3]	Fig. 8(a)	Passive	10.0	71.6	0.4740	1.00 $\langle \varepsilon \rangle$		A	
				65.3	0.0633	1.00 $\langle \varepsilon \rangle$		B	
				60.7	0.0174	1.00 $\langle \varepsilon \rangle$		C	
	Fig. 8(a)	Passive	10.0	48.6	0.7540	1.15 $\langle \varepsilon \rangle$		D	
				41.1	0.0731	1.15 $\langle \varepsilon \rangle$		E	
				38.1	0.0145	1.25 $\langle \varepsilon \rangle$		F	
				36.6	0.00485	1.25 $\langle \varepsilon \rangle$		G	
Yeh and Van Atta [16]	Figs. 2, 3	Passive	4.06	35.2	0.0456	0.154	0.90 $\langle \varepsilon \rangle$	0.90 $\langle \chi \rangle$	H
Schedvin <i>et al.</i> [13]	Fig. 6	Passive	28.9	280	2.2 $\pm$ 0.3		1.15 $\langle \varepsilon \rangle$		I
Sepri [14]	Figs. 6, 7	Passive	4.0	35	0.0282	0.158	1.35 $\langle \varepsilon \rangle$	0.55 $\langle \chi \rangle$	J
Warhaft and Lumley [15]	Figs. 4, 10	Passive	6.5	$\sim$ 45	0.0951	0.0279	1.25 $\langle \varepsilon \rangle$	0.95 $\langle \varepsilon \rangle$	K
Mydlarski and Warhaft [9]	Fig. 4	Active (random)	7.1	262	1.06	1.15 $\langle \varepsilon \rangle$		L	
	Fig. 8	Active (random)	14.3	473	15.3	1.25 $\langle \varepsilon \rangle$		M	
	Fig. 8	Passive	7.3	100	0.0708	1.20 $\langle \varepsilon \rangle$		N	
	Fig. 8	Passive	7.6	50	0.227	1.15 $\langle \varepsilon \rangle$		O	
	Fig. 22	Active (random)	10.4	377	4.54	1.30 $\langle \varepsilon \rangle$		P	
Mydlarski and Warhaft [10]	Fig. 3	Active (random)	7.0	582	0.94	1.74	0.65 $\langle \varepsilon \rangle$	0.55 $\langle \chi \rangle$	Q
	Fig. 3	Active (synchronous)	6.0	247 (217)	0.164	0.581	0.70 $\langle \varepsilon \rangle$	0.70 $\langle \chi \rangle$	R
	Fig. 20	Active (synchronous)	3.3	140	0.0418	0.277	1.10 $\langle \varepsilon \rangle$	0.60 $\langle \chi \rangle$	S
Larssen and Devenport [7]	Fig. 5	Active (random)	Case 39	20.2	1362	16.46	1.15 $\langle \varepsilon \rangle$		1
			Case 8	19.2	1053	6.06	1.15 $\langle \varepsilon \rangle$		2
			Case 7	15.1	919	2.63	1.20 $\langle \varepsilon \rangle$		3
			Case 12	14.8	722	2.95	1.15 $\langle \varepsilon \rangle$		4
			Case 11	12.7	664	1.44	1.20 $\langle \varepsilon \rangle$		5
			Case 5	8.6	599	0.42	1.20 $\langle \varepsilon \rangle$		6
			Case 10	10.7	565	0.91	1.15 $\langle \varepsilon \rangle$		7

- [5] Djenidi, L. and Antonia, R. A., A spectral chart method for estimating the mean turbulent kinetic energy dissipation rate, *Exp. Fluids*, **53**, 2012, 1005–1013.
- [6] Kolmogorov, A. N., The local structure of turbulence in incompressible viscous fluid for very large Reynolds numbers [1991 English translation in Proc. Roy. Soc. Lond. Ser. A Math. Phys. Sci. 434(1890):9–13], *Dokl. Akad. Nauk SSSR*, **30**, 1941, 299–303.
- [7] Larssen, J. V. and Devenport, W. J., On the generation of large-scale homogeneous turbulence, *Exp. Fluids*, **50**, 2011, 1207–1223.
- [8] Lee, S. K., Benaissa, A., Djenidi, L., Lavoie, P. and Antonia, R. A., Scaling range of velocity and passive scalar spectra in grid turbulence, *Phys. Fluids*, **24**, 2012, 075101.
- [9] Mydlarski, L. and Warhaft, Z., On the onset of high-Reynolds-number grid-generated wind tunnel turbulence, *J. Fluid Mech.*, **320**, 1996, 331–368.
- [10] Mydlarski, L. and Warhaft, Z., Passive scalar statistics in high-Péclet-number grid turbulence, *J. Fluid Mech.*, **358**, 1998, 135–175.
- [11] Obukhov, A. M., The structure of the temperature field in a turbulent flow, *Izv. Akad. Nauk SSSR, Ser. Geogr. Geofiz.*, **13**, 1949, 58–69.
- [12] Pope, S. B., *Turbulent flows*, Cambridge University Press, Cambridge, 2000.
- [13] Schedvin, J., Stegen, G. R. and Gibson, C. H., Universal similarity at high grid Reynolds numbers, *J. Fluid Mech.*, **66**, 1974, 561–579.
- [14] Sepri, P., Two-point turbulence measurements downstream of a heated grid, *Phys. Fluids*, **19**, 1976, 1876–1884.
- [15] Warhaft, Z. and Lumley, J. L., An experimental study of the decay of temperature fluctuations in grid-generated turbulence, *J. Fluid Mech.*, **88**, 1978, 659–684.
- [16] Yeh, T. T. and Van Atta, C. W., Spectral transfer of scalar and velocity fields in heated-grid turbulence, *J. Fluid Mech.*, **58**, 1973, 233–261.
- [17] Zhou, T., Antonia, R. A., Danaila, L. and Anselmet, F., Transport equations for the mean energy and temperature dissipation rates in grid turbulence, *Exp. Fluids*, **28**, 2000, 143–151.